Title: *Salmonella* relies on siderophore exploitation at low pH

Authors: Manon Ferry[1], Isabelle J. Schalk[1] and Olivier Cunrath[1*]

Affiliation: [1] CNRS, UMR7242, Biotechnology and cell signaling, University of Strasbourg, Illkirch, France;

[*] Correspondence to: olivier.cunrath@unistra.fr

Abstract

Salmonella enterica, a prominent enteric pathogen, employs sophisticated iron acquisition mechanisms to overcome host-imposed iron limitation, notably through the production and uptake of siderophores—small, high-affinity iron-chelating compounds that scavenge iron from the host environment. In this study, we investigate how environmental pH influences *Salmonella's* preference for its endogenous siderophores versus exogenous siderophores within the physiological range of the gastrointestinal tract. Through competition assays, gene expression analysis, and siderophore quantification, we demonstrate that *Salmonella* increasingly relies on exogenous siderophores under acidic conditions. This shift is attributed to reduced production of its endogenous siderophores, enterobactin and salmochelin. Deletion of the sigma factor RpoS enhances endogenous siderophore production and iron acquisition at low pH, suggesting its role in regulating iron homeostasis. Our findings reveal a pH-dependent adaptation in *Salmonella's* iron acquisition strategy, highlighting the pathogen's versatility in nutrient acquisition across varying gastrointestinal conditions. This research provides insights into *Salmonella's* pathogenicity and may inform the development of targeted interventions for *Salmonella* infections.

Keywords

pH-dependent siderophore exploitation, *Salmonella*, siderophores, gut, regulation, *fhuA*, *foxA*, *foxR*, *fur*, *rpoS*

Introduction

Iron is a vital nutrient for all organisms, playing a key role as a cofactor in enzymes that drive growth and metabolism[1]. However, iron bioavailability is limited in many environments, making it a scarce resource for both the host and invading pathogens[2–4]. During infection, the host organism mounts a defense strategy known as nutritional immunity, which tightly restricts the levels of available iron, effectively limiting its accessibility to pathogens[5,6]. By limiting access to iron, the host forces pathogens to compete for this essential resource. This competition shapes the course of infection and drives pathogens to develop various strategies for acquiring the iron they need to survive and proliferate. One of these strategies is the production of siderophores—high-affinity molecules that scavenge iron from the environment and facilitate its uptake into bacterial cells[7]. Siderophores are synthesized by various microorganisms in response to iron scarcity and are secreted into the extracellular environment, where they form stable complexes with iron[8]. Once the siderophore-iron complex is formed, it is recognized and actively transported back into the microbial cell via specific transport systems. These transporters, located on the microbial surface, are highly selective and efficiently bring the iron-bound siderophore inside the cell, where the iron is released for cellular use[9].

Numerous studies highlight the essential role of siderophores in the inflamed intestinal environment[10–13]. The host actively interferes with bacterial siderophore utilization by producing molecules like lactoferrin, transferrin and calprotectin, which tightly bind iron,

limiting its availability to pathogens[14–16]. Additionally, the secretion of lipocalin-2 further restrict microbial access to iron, by capturing some iron-loaded siderophores[17]. Beyond the host's defense mechanisms, the gut microbiota plays an additional role in the competition for iron. Certain commensal bacteria, such as *Lactobacillus* and *Bifidobacterium* species, along with some fungal strains like *Aspergillus* and *Malassezia*, are known to produce their own siderophores to acquire iron[18–21]. Siderophores can also enter the intestinal environment through the diet, as they are produced by microorganisms naturally found in fermented foods[21,22]. Together, these factors suggest that the intestinal environment is a dynamic landscape where iron is bound to a variety of siderophores. To thrive in this complex setting, many bacteria have evolved not only to produce their own siderophores but also to exploit exogenous siderophores — siderophores produced by other organisms and present in their environment (also referred to as xenosiderophores) [23–25]. For instance, commensal gut bacteria such as *Bacteroides* can exploit siderophores produced by other microorganisms, as can gut pathogens like *Candida albicans*, *Clostridioides difficile*, and *Escherichia coli*[26–29]. This dual capability to both produce and exploit siderophores provides pathogens with a versatile strategy to navigate the diverse ecological niches of the gut. To explore how these strategies may influence pathogen proliferation, we focus on *Salmonella enterica enterica* serovar Typhimurium, a prominent model pathogen of gastrointestinal infections and iron homeostasis[13].

Salmonella is capable of producing two catecholate-type siderophores—enterobactin (ENT), through the biosynthetic gene cluster EntCEBAH[30,31], and salmochelin (SLC), its C-glucosylated derivative, through glycosylation mediated by the IroB enzyme[32]—in response to iron scarcity[33]. Of all reported siderophores so far, ENT exhibits the highest affinity for iron ($K_a = 10^{49}\ M^{-1}$)[34] but can be neutralized by the host protein lipocalin-2, which sequesters ENT, thus blocking this iron acquisition pathway[17]. In contrast, the glycosylation of SLC ($K_a = 10^{45}$

74 M^{-1})[12] prevents recognition by lipocalin-2, allowing *Salmonella* to evade this immune defense
75 while maintaining its high affinity iron acquisition system, even under conditions of severe
76 iron limitation[35].

77 As for all Gram negative bacteria, ferri-siderophore complexes formed in the bacterial
78 environment cross the outer membrane through TonB-dependent transporters (TBDTs),
79 utilizing energy derived from the proton motive force transmitted by the TonB-ExbB-ExbD
80 inner membrane complex[36–40]. TBDTs are highly specific to their ligand, ensuring selective
81 uptake of the iron-loaded siderophores (recently reviewed here[8,13]). In *Salmonella*, ferric-ENT,
82 ferric-SLC, and their ferric break-down products 2,3-dihydroxybenzoylserine (DHBS) are
83 recognized by specific the following TBDTs: FepA for ENT and DHBS, IroN for SLC and
84 DHBS, and CirA for DHBS (Fig. 1, left part)[31,41,42]. Beyond producing its own endogenous
85 siderophores, *Salmonella* can also exploit three exogenous siderophores found in its
86 environment: ferrichrome (FC) ($K_a = 10^{29}$ M^{-1})[23,43], coprogen (CPG) ($K_a = 10^{27}$ M^{-1})[36,44], and
87 ferrioxamines (DFO) ($K_a = 10^{32}$ M^{-1})[37,45], all of which are hydroxamate-type siderophores
88 (Figure 1, right part). This specialized transport mechanism enables *Salmonella* to efficiently
89 acquire iron from the environment, particularly under iron-limited conditions, by facilitating
90 the uptake of the strong affinity ferric-siderophore complexes.

91 Genes encoding siderophore transporters or involved in their biosynthesis are
92 negatively regulated by the ferric uptake regulator Fur, a globally conserved transcriptional
93 regulator that controls iron homeostasis in bacteria[46]. Fur functions as a repressor by binding
94 to specific DNA sequences known as Fur boxes located in the promoter regions of target genes
95 when complexed with Fe^{2+}. In addition to the regulation by Fur, certain genes involved in
96 siderophore acquisition are controlled by other mechanisms. For example, the TBDT FoxA,
97 responsible for ferrioxamine E (DFOE) uptake, exhibits a ligand-specific upregulation

98 mechanism mediated by the AraC-type transcriptional regulator FoxR. FoxR binds to DFOE
99 in the cytoplasm, activating the transcription of the *foxA* gene and thereby upregulating FoxA
100 expression to improve *Salmonella*'s access to this exogenous siderophore (Fig. 1, right part),
101 thus optimizing the bacterial iron acquisition process under iron-limited conditions[47].

102 Our understanding of how pathogens selectively use siderophores under various
103 infection conditions remains limited. One key question is whether pathogens primarily rely on
104 the production of their own siderophores or whether they exploit exogenous ones, and how this
105 choice is influenced by the dynamic conditions of the intestinal environment. Environmental
106 factors such as changes in pH, which fluctuate within the gut, could significantly impact iron
107 availability and may affect the way siderophores are utilized[39,48–50]. Given the energetic cost of
108 siderophore production and the nutrient restrictive environment imposed by both the host and
109 the innate microbiome, it is plausible to assume that, under certain conditions, pathogens might
110 favor the exploitation of exogenous siderophores[51]. This raises important questions about the
111 adaptive mechanisms' pathogens employ to optimize their iron acquisition in the face of a
112 constantly shifting gut environment. Here we show that siderophore exploitation is a vastly
113 conserved strategy among all tested *Salmonella* sub-populations. We further show that
114 exogenous siderophore exploitation is key for *Salmonella's* survival during iron starvation at
115 low pH. Despite complex regulatory mechanisms involved in iron homeostasis, we find that
116 this pattern can be explained by a simple underlying principle: a stark reduction of the
117 endogenous siderophore production in acidic conditions. Furthermore, we have shown that this
118 down-regulation may represent a pathogen's weakness that can be utilized for better pathogen
119 control strategies[21,52–54].

120

121

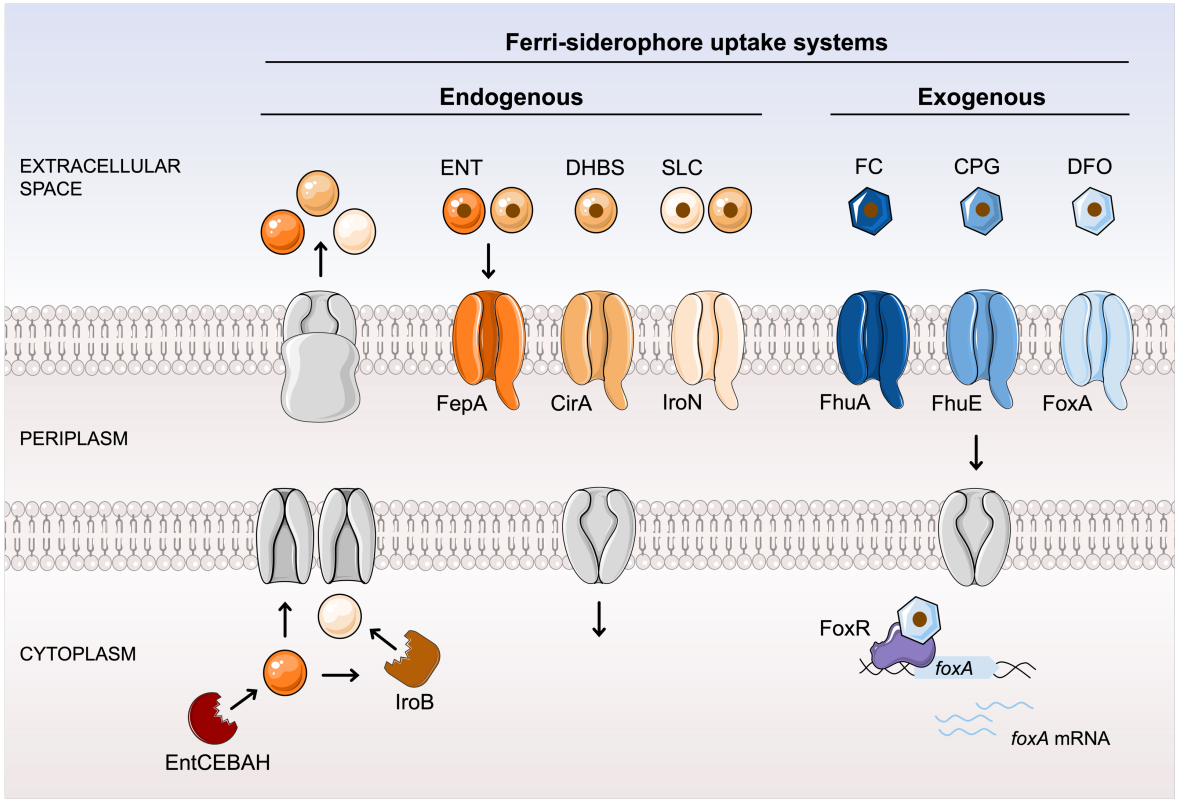

Figure 1. Siderophore mediated iron uptake in *Salmonella enterica*. Schematic diagram illustrating the pathways for the acquisition of endogenous (left) and exogenous (right) siderophores identified in *S. enterica* Typhimurium. Iron (brown circle) is captured from the extracellular environment and the ferri-siderophore complex is transported into the cell by TBDTs. Endogenous siderophores, produced by the *entCEBAH* operon, include ENT (dark orange circle), its break-down product DHBS (medium orange circle), and SLC (light orange circle). SLC is a glycosylated derivative of ENT, with glycosylation facilitated by IroB. All three are recognized by TBDTs FepA, IroN, and CirA. Exogenous siderophores—FC (dark blue hexagon), CPG (medium blue hexagon), and DFO (light blue hexagon)—are imported by TBDTs FhuA, FhuE, and FoxA, with FoxA being positively regulated by the cytoplasmic regulator FoxR.

Results

Siderophore uptake systems are very conserved suggesting key ecological roles in *Salmonella enterica* lifestyle

Salmonella enterica is well known for its ability to both produce its own siderophore and exploit exogenous siderophores. *Salmonella* is able to synthesize ENT through the biosynthetic gene cluster EntCEBAH[30,31] and SLC through a glycosylation of ENT mediated

141 by the IroB enzyme[32]. ENT, SLC, and their break down product DHBS are recognized by
142 specific TBDTs: FepA for ENT and DHBS, IroN for SLC and DHBS, and CirA for
143 DHBS[31,41,42]. To assess the conservation of *Salmonella's* endogenous siderophore uptake
144 systems we analyzed siderophore-related genes in 183 *S. enterica* strains. These strains were
145 randomly chosen with one strain selected for each unique multilocus sequence typing (MLST)
146 profile on the PATRIC database using Python's *random.choice()* function to ensure a diverse
147 dataset[55]. Our results reveal a strong conservation of all endogenous siderophore biosynthesis
148 and uptake systems across the species (Fig. 2). Nearly all strains possess
149 the *entC* and *fepA* genes (>99%), which enable the biosynthesis and uptake of ENT,
150 respectively, highlighting the importance of these genes in *Salmonella*'s iron acquisition
151 strategies. Likewise, *cirA* is universally present, supporting the consistent use of this
152 transporter across strains. Furthermore, the high conservation of both *iroB* and *iroN* (98.9%)
153 in almost all strains suggest a strong conservation of the capacity to produce and import SLC.

154 In addition to its own siderophores, *Salmonella* can exploit exogenous siderophores
155 present in its environment, such as FC, CPG, and DFO. These are imported via other TBDTs:
156 FhuA for FC, FhuE for CPG, and FoxA for DFO[36,37,39]. Recent research has further
157 demonstrated the regulatory role of the AraC-type regulator FoxR in enhancing DFOE
158 uptake[47]. When analyzing the conservation of genes encoding for exogenous siderophore
159 TBDTs as described above, we could show that although their conservation was slightly more
160 variable than for the endogenous transporters, conservation still remains high (Fig. 2).
161 The *fhuA* gene, responsible for FC transport, is slightly less conserved but is still present in
162 about 73% of the strains. Conversely, the genes for CPG and DFO transport—*fhuE* (> 99%)
163 and *foxA* (94%), respectively—are highly conserved, as is *foxR* (95%), the positive regulator
164 of *foxA*. All but one strain possesses at least one exogenous siderophore transporter,
165 underscoring the species-wide dependency to access exogenous siderophores in diverse

environments (Fig. 2). A broader analysis of approximately 1,200 strains with unique genomes showed the same trend, reinforcing the conclusion that siderophore-dependent iron uptake systems are highly conserved across the species and likely play a key role in *Salmonella*'s infection process (fig. S1; Tab S5).

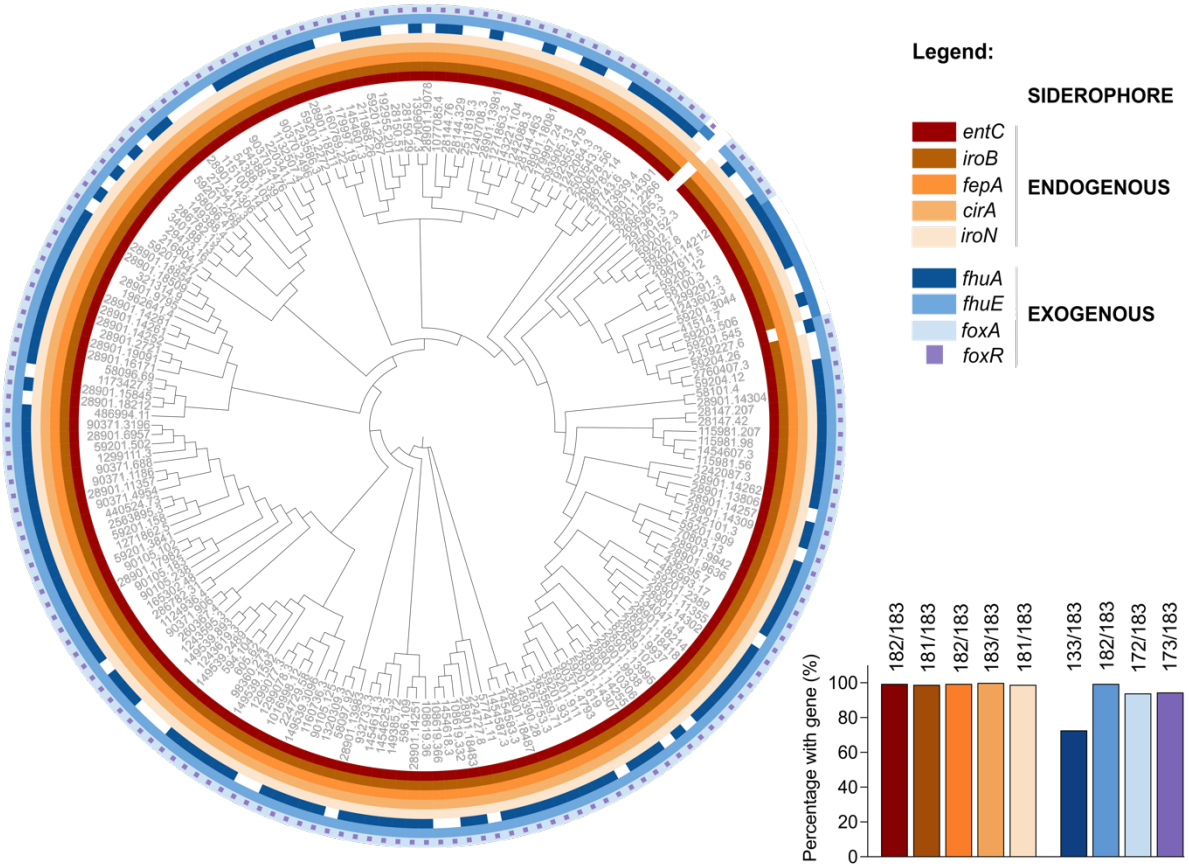

Figure 2. Conservation of siderophore-related genes across *Salmonella enterica* species highlights their ecological importance. Phylogenetic tree of 183 *Salmonella* strains. The phylogeny is based on the core gene alignment of all strains, selected to maximize genetic diversity with each having a unique MLST profile. Circles around the tree depict the presence or the absence of specific genes, with each circle corresponding to one gene. Colored rectangles next to each strain's Genome ID (PATRIC BV-database) indicate gene presence, while white rectangles show absence. The histogram shows the percentage of strains that possess each studied gene.

The reliance of *Salmonella* on exogenous siderophore exploitation increases in acidic conditions

183 Changes in pH within the gastrointestinal tract can significantly affect siderophore
184 physicochemical properties[48,56]. As the pH fluctuates, the chelating properties of siderophores
185 may be modified, which in turn may influence their relative importance in iron acquisition. For
186 example, ENT, a catecholate-type siderophore, sees its affinity strongly decrease upon
187 acidification of the environment, due to protonation of the catechol groups [34,48]. On the other
188 hand, hydroxamate siderophores like deferoxamine (DFO) depict a weaker affinity for iron at
189 neutral pH but show a weaker decrease in affinity upon acidification[48,57]. Given this pH-
190 dependent variability in siderophore affinity, we hypothesize that acidic conditions in the gut
191 could influence *Salmonella*'s preference towards exploiting exogenous hydroxamate
192 siderophores, as their uptake might be less affected by the changes in iron affinity compared to
193 their endogenous siderophore ENT.

194 To investigate the influence of pH on *Salmonella*'s use of exogenous siderophores, we
195 performed bacterial competition assays (Fig. 3A). In these assays we investigated two different
196 exogenous siderophores uptake systems; the FC uptake, in which the transcription and
197 consequently the expression of the TBDT FhuA is solely regulated by the general iron regulator
198 Fur, and the iron uptake by DFOE, where the transporter FoxA has its expression regulated by
199 Fur and is also inducible by the presence of the DFOE via FoxR (Fig. 1)[37,47]. A WT strain and
200 an isogenic strain lacking the gene encoding for the exogenous-siderophore transporter (*fhuA*
201 or *foxA*) or the regulator (*foxR*) were co-cultured in iron-depleted media at various pH levels,
202 with increasing concentrations of the corresponding exogenous siderophores. It is important to
203 note that both competing strains were capable of producing and using their endogenous
204 siderophores to acquire iron. For each condition, we measured the competitive index (CI) of
205 the mutant strain relative to the WT strain (as calculated by the CFU ratio (mutant/WT) at 48h
206 divided by the CFU ratio (mutant/WT) of the inoculum) to assess the advantage conferred by
207 the ability to exploit exogenous siderophores across different pH levels (Fig. 3A). These

208 experiments showed a decreased fitness of the mutant strain in increasing concentrations of our
209 exogenously added siderophores (Fig. 3BCD). At intermediate concentration such as 0.1 μM
210 this decrease was significantly more pronounced at low pH. Therefore, our results showed a
211 significant pH-dependent effect on the advantage provided by FC exploitation (Fig. 3B). The
212 inability to use FC, due to the deletion of *fhuA*, demonstrated that *Salmonella* gains a distinct
213 advantage from FC exploitation more quickly in acidic conditions than at neutral pH. Similarly,
214 when comparing the WT strain that can use DFOE to the *foxA* mutant strain that cannot, we
215 observed the same pH-dependent advantage (Fig. 3C). Since FoxA appears more important
216 under acidic conditions, we investigated the relative advantage of FoxR-mediated upregulation
217 of the FoxA transporter. Our findings indicate that, in the presence of all tested concentrations
218 of DFOE, FoxR-mediated upregulation is only relevant for *Salmonella* in acidic conditions
219 (Fig. 3D). Growth assays revealed a striking pH-dependent role for FoxR. At neutral pH, a
220 *foxR* mutant grows similarly to WT, even in the presence of 10 μM of DFOE, indicating that
221 FoxR is dispensable under these conditions (fig. S2). In contrast, at acidic pH, the same *foxR*
222 mutant exhibits a significant growth defect compared to WT when DFOE is present,
223 demonstrating that FoxR is essential for *Salmonella's* fitness in acidic environments (fig. S2).
224 The same findings also hold in an *entC* mutant background, unable to produce its own
225 siderophore (fig. S3). These findings reveal that acidic pH represents a condition in which the
226 regulator FoxR becomes crucial for iron acquisition. At low pH, *Salmonella* requires both the
227 FoxA transporter and its up-regulation by FoxR to effectively exploit DFOE siderophore;
228 without which siderophore exploitation may be blocked.

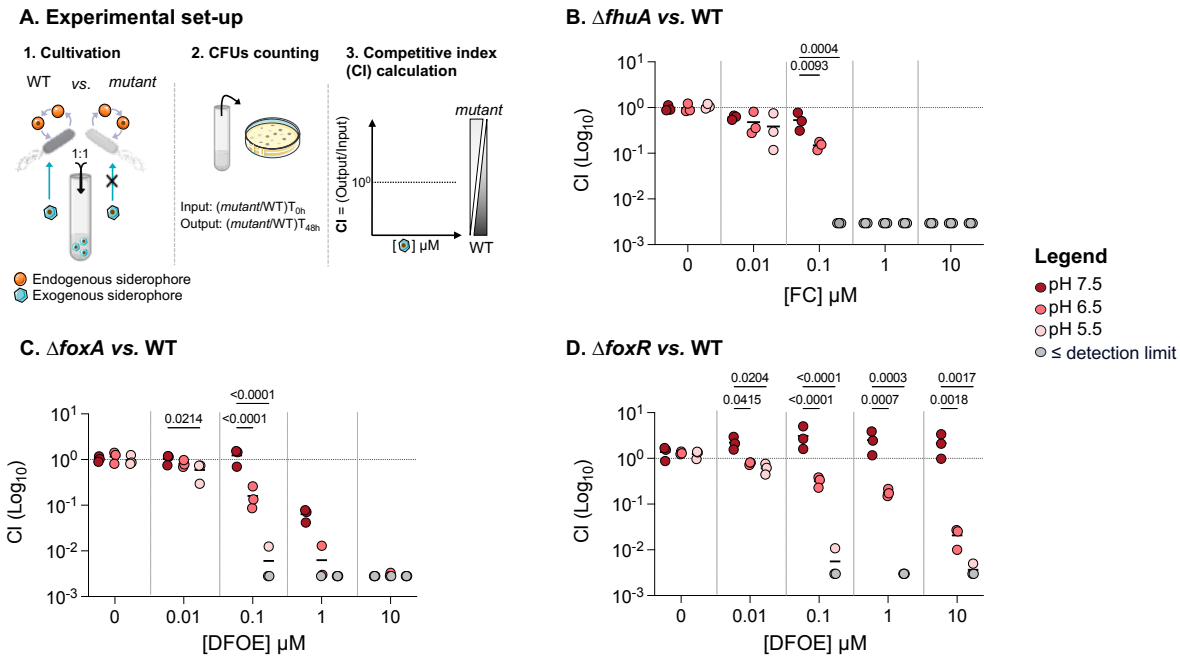

Figure 3. The reliance of *Salmonella* on exogenous siderophore exploitation increases in acidic conditions. A. Experimental setup for competition assays. Two fluorescently labeled *Salmonella* strains are mixed in equal amounts, with one strain unable to utilize the exogenous siderophore. Cultures are grown in Minimal Medium (MM) with or without the exogenous siderophore. After 48 hours, the ratio of mutant to wild-type colonies is determined by plating on selective agar, and the competitiveness index (CI) is calculated (for more details the Method section). A CI > 1 indicates a competitive advantage for the mutant strain, while a CI < 1 indicates an advantage for the wild-type strain. **B.** Competitive indexes of Δ*fhuA* s *vs*. WT strain in presence of FC. **C.** Competitive indexes Δ*foxA vs*. WT strain in presence of DFOE. **D.** Competitive indexes of Δ*foxR vs*. WT strain –regulator of FoxA in presence of DFOE. All assays were performed in MM at pH 7.5 (dark red), 6.5 (medium red), or 5.5 (light red), with or without increasing concentrations of exogenous siderophores. The output ratio was calculated after 48 hours of culture. Each data point represents one biological replicate (n = 3). Points below the detection limit for each assay are shown in gray. Statistical analysis was performed using one-way ANOVA followed by Tukey's multiple comparisons test. Exact p-values are reported for all comparisons with $p < 0.05$ considered statistically significant.

Reduced endogenous siderophore production increases dependence on exogenous siderophores in acidic conditions

While the affinity between iron and the siderophore varies at different pH, we explored if our pH-dependent phenotype could be explained by more than just the affinity difference between iron and the siderophores[48]. TBDTs that import siderophores are highly specific, with

252 each transporter recognizing a particular siderophore-iron complex[8]. Previous studies have
253 shown that pH can alter the affinity of the siderophore-iron complex for its transporter[51]. To
254 understand why *Salmonella* gains a significant growth advantage from exogenous siderophore
255 utilization in acidic conditions, we examined whether pH affects the affinity of the siderophore-
256 iron complex for its transporter. Therefore, we measured the affinity of Fe-DFOE, one of the
257 three exogenous siderophores utilized by *Salmonella*, for its transporter FoxA. Specifically,
258 *Salmonella* cells expressing FoxA were incubated with increasing concentrations of
259 radiolabeled ^{55}Fe-DFOE at 4°C. At this temperature, Fe-siderophores bind to their TBDT but
260 no uptake into the bacteria occurs[58]. After incubation, unbound complexes were removed by
261 filtration and the radioactivity associated with the bacterial pellet was measured by scintillation
262 counting. These data were used to generate binding curve and calculate the dissociation
263 constant (K*d*), providing a quantitative measure of the interaction between Fe-DFOE and
264 FoxA. Our findings indicate that the growth advantage is not due to changes in siderophore
265 binding properties, as DFOE displayed consistent affinity for its transporter FoxA at both pH
266 7.5 and 5.5 with dissociation constants of around 3.2 ± 7.6 nM and 3.2 ± 11.0 nM, respectively
267 (fig. S4).

268 Another possibility is that the increased dependence on exogenous siderophore under
269 acidic condition could be attributed to modifications in bacterial physiology induced by pH.
270 The expression profile of the *ryhB2* reporter —a small regulatory RNA involved in iron
271 homeostasis— across our pH range (5.5, 6.5, 7.5) indicates that the bacterial iron requirement
272 is reduced in acidic environments. This may partly explain the downregulation of siderophore
273 systems observed under these conditions, while also confirming that all tested conditions
274 remain iron-deleted (fig. S5). We then explored two possible scenarios to explain the increased
275 reliance on exogenous siderophores: either exogenous uptake systems are more highly
276 expressed in acidic environments, or endogenous uptake systems are less expressed, leading to

277 greater dependence on exogenous siderophore exploitation. To assess the expression levels of
278 siderophore-uptake pathways in relation to pH, we used plasmid-encoded fluorescent
279 transcriptional reporter fusions[59,60] in which we have cloned the promoter region of the gene
280 of interest in front of GFP.

281 Using this approach, we observed a reduction in the transcription of the exogenous *foxA*
282 and *fhuA* genes under acidic conditions, even when grown in the presence of their respective
283 ligand (Fig. 4A). We then investigated the expression of genes involved in the endogenous
284 siderophore uptake system (Fig. 4B). Specifically, the expression of the *entCEBAH* operon,
285 which is responsible for ENT production, and *iroB*, which contributes to SLC production, was
286 also reduced in acidic conditions. Similarly, the expression of endogenous siderophore TBDTs
287 such as *cirA*, *fepA*, and *iroN* decreased, suggesting that endogenous siderophores are produced
288 at lower levels in acidic conditions. This was further supported by the quantification of
289 endogenous siderophores using UV-visible spectroscopy, which revealed reduced
290 concentrations of endogenous siderophores (ENT/SLC and DHBS) in the supernatant of strains
291 cultivated under acidic conditions (Fig. 4C). To make sure that this phenomenon is not strain-
292 specific, we quantified ENT/SLC and DHBS production in various phylogenetically diverse
293 *Salmonella* strains, which reveal similar trends (fig. S6). In addition to the use of siderophores,
294 *Salmonella* also possesses ferrous iron uptake systems such as FeoABC, SitABCD and MntH
295 [61–63] (recently reviewed here[13]). To investigate if those system may be of greater importance in
296 acidic conditions, we also examined whether the expression of the three major ferrous iron
297 import systems are upregulated under acidic conditions. However, our results indicate that
298 these import systems are not significantly more expressed in acidic environments compared to
299 neutral ones (fig. S7). Taken together, these findings suggest that, under acidic
300 conditions, *Salmonella* shifts toward a greater reliance on exogenous siderophores due to
301 reduced production of its own endogenous siderophores and a change in iron-chelating affinity.

302 At neutral pH, ENT/SLC siderophores have a higher affinity for iron than hydroxamate
303 siderophores, but at acidic pH, their affinity decreases to a level comparable to that of
304 hydroxamates, making them less competitive in acidic conditions[48]. In our competition model,
305 hydroxamate siderophores are already present in the environment, which may further
306 enhance *Salmonella*'s dependence on these exogenous siderophores to access iron. This
307 combination of limited production and reduced affinity in acidic conditions likely
308 drives *Salmonella* to favor exogenous siderophore uptake. To test whether this increased
309 reliance is indeed due to reduced endogenous siderophore production, we supplemented the
310 culture medium with pure ENT to see if this addition could alleviate the dependence on
311 exogenous sources (Fig. 4D). We competed a WT strain with a strain deficient in DFOE uptake
312 (*foxA* mutant) at both pH 7.5 and 5.5. While the addition of DFOE alone conferred a growth
313 advantage to the WT strain in acidic conditions, this advantage was lost when the same
314 concentration of ENT was added alongside DFOE. The presence of exogenous ENT effectively
315 reduces *Salmonella*'s reliance on exogenous siderophores, highlighting the critical role of
316 endogenous siderophore production in facilitating growth under acidic conditions.

317 Our results indicate that *Salmonella*'s increased reliance on exogenous hydroxamate-
318 type siderophore exploitation under acidic conditions is driven by a combination of factors.
319 The decreased production of endogenous catechol siderophores, combined with the reduced
320 affinity of *Salmonella*'s endogenous siderophores for iron in acidic environments, drives a
321 greater dependence on exogenous sources of siderophores.

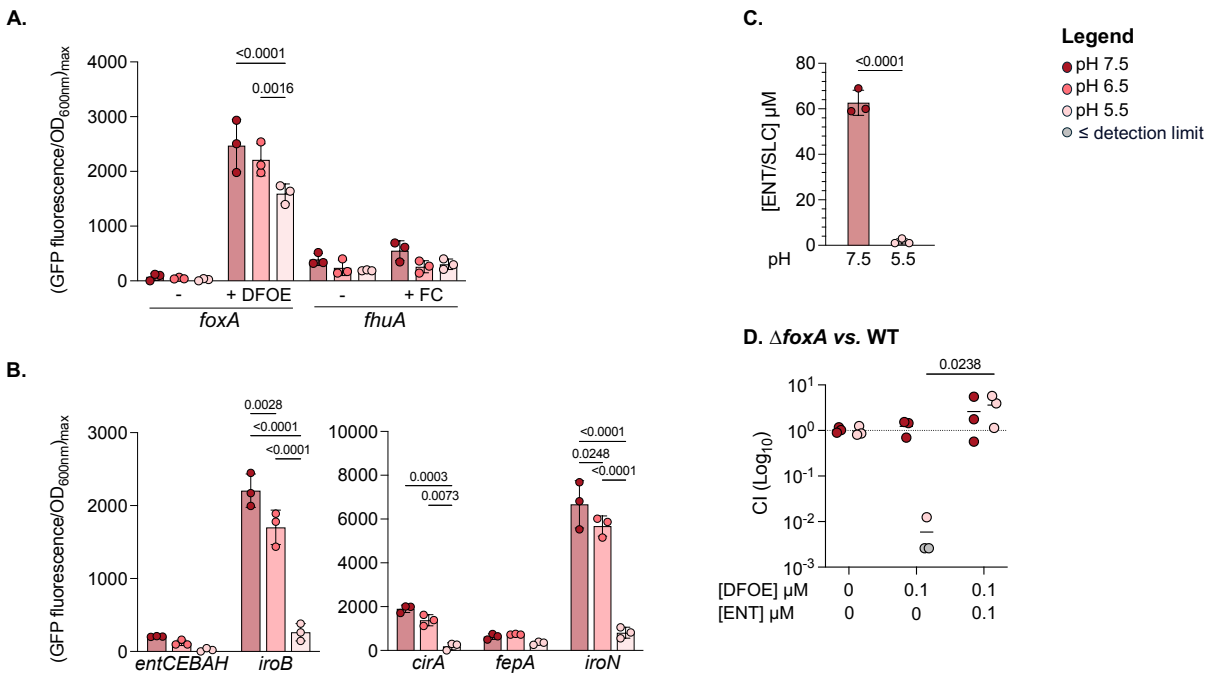

Figure 4. Endogenous siderophore production decreases in acidic conditions, heightening reliance on exogenous siderophores. A-B. Transcriptional expression of siderophore-related genes. WT strains carrying plasmid encoded fluorescent reporters were cultivated in MM at pH 7.5 (dark red), 6.5 (medium red), or 5.5 (light red). GFP-fluorescence emission data, normalized to optical density at 600 nm (OD_{600nm}) of the culture, are shown as the maximum fluorescence per OD_{600nm}. Each point represents a biological replicate. **A.** Expression levels of genes encoding exogenous siderophore transporters with or without 10 µM of their respective ligand. **B.** Expression levels of genes encoding transporters and enzymes involved in the biosynthesis of endogenous siderophores. **C**. Concentration of endogenous siderophores (ENT/SLC, and DHBS) in the supernatant of WT *Salmonella* cultures after 24 hours of cultivation in MM at pH 7.5 (dark red) and 5.5 (light red). The concentrations of ENT and SLC are shown together, as they have similar spectral properties, with SLC being a glycosylated derivative of ENT. **D.** Competitive indexes of Δ*foxA vs.* WT strain at pH 7.5 5 (dark red) and 5.5 (light red). The competition was conducted in MM with no supplementation, 0.1 µM DFOE, or 0.1 µM DFOE plus 0.1 µM ENT. The output ratio was calculated after 48 hours of culture. Each data point represents one biological replicate (n = 3). Points below the detection limit for each assay are shown in gray. Statistical analysis was performed using one-way ANOVA followed by Tukey's multiple comparisons test (A, B, D) or unpaired t-test (C). Exact p-values are reported for all comparisons with $p < 0.05$ considered statistically significant.

Loss of the sigma factor RpoS enhances endogenous siderophore production and acquisition at acidic pH

To elucidate the regulatory mechanisms underlying the reduced production of endogenous siderophores in acidic conditions, we investigated the roles of two potential

347 candidates: Fur and RpoS (σ^{70}). Fur is a key regulator of iron homeostasis in *Salmonella*,
348 typically repressing iron import systems when iron is plentiful[46]. RpoS, a sigma factor, is
349 involved in the transcription of genes associated with stress responses[64,65]. Given that our
350 experimental conditions are both iron-poor and acidic, both Fur and RpoS were considered
351 promising candidates for this study. Notably, the stress sigma factor RpoS has been shown to
352 counteract Fur's repression of genes involved in iron and manganese metabolism and modulate
353 the metallome of *Salmonella enterica* serovar Typhimurium[66]. This suggests a potential
354 regulatory interplay between Fur and RpoS in response to environmental stressors such as
355 acidic conditions, where both factors could play a role in modulating iron homeostasis and
356 siderophore production.

357 We measured endogenous siderophore concentrations in the supernatants of strains
358 grown at pH 7.5 and 5.5 for both *fur* and *rpoS* mutant (Fig. 5A and fig. S5). The deletion
359 of *fur* did not increase siderophore production. The fact that the depletion of Fur does not
360 significantly impact siderophore production under our iron-limited conditions, suggests that in
361 all our growth conditions Fur is completely de-repressed. While iron requirements may be
362 reduced at low pH, *Salmonella* is still facing strict iron deprivation, highlighting the persistent
363 iron limitation even under acidic stress. In contrast, the deletion of *rpoS* led to a marked
364 increase in the concentration of endogenous siderophores in the growth medium, particularly
365 at low pH, where the increase in ENT levels was significantly more pronounced than in the
366 WT strain. At neutral pH, the difference was also evident, but the effect was far greater under
367 acidic conditions (1.5-times more ENT at pH 7.5 versus 60-times more ENT at pH 5.5).
368 Additionally, the *rpoS* mutant showed an enhanced iron deficiency response, as indicated by
369 the increased expression of the small RNA *ryhB2* in all three pH conditions tested (Fig. 5B and
370 fig. S5). This upregulation was also observed for genes related to both endogenous and
371 exogenous siderophore import, such as *entCEBAH*, *fepA*, and *foxA* (Fig. 5C - 5E and fig. S5).

RpoS is known to modulate nutrient acquisition, typically by repressing the expression of various nutrient uptake systems. While at neutral pH iron-uptake systems are already active, the absence of RpoS has only limited effects on siderophore production. Contrary, at low pH, the absence of RpoS results in a more significant effect, where ENT production is strongly increased. This enhanced production of ENT at low pH underscores the stronger iron acquisition capacity in the *rpoS* mutant under these conditions. RpoS seems to have a significant role in regulating siderophore production under acidic conditions, whether directly or through intermediary pathways, leading to a drastic effect on growth under iron starvation.

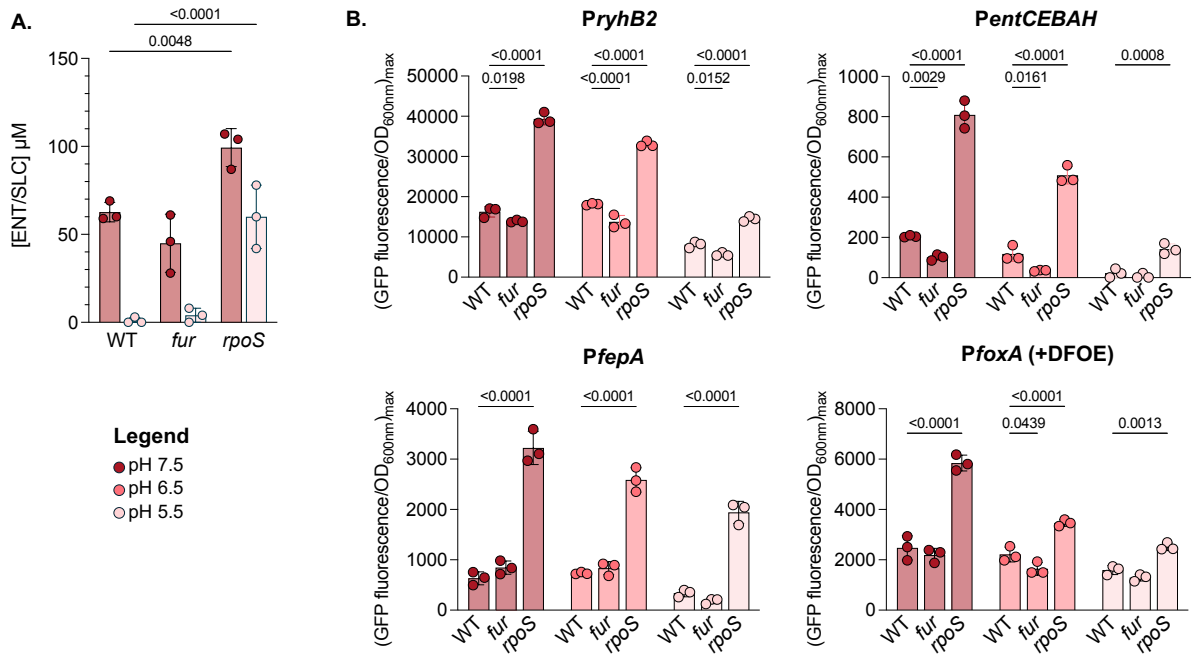

Figure 5. Loss of the sigma factor RpoS enhances endogenous siderophore production and acquisition at acidic pH. A. Measurement of endogenous siderophore production (ENT/SLC) in the Δ*fur* and Δ*rpoS* mutants grown in MM at pH 7.5 (dark red) and 5.5 (light red). Siderophore concentrations were quantified from the supernatant after 24 hours of cultivation (n = 3). **B-E.** Transcriptional expression of siderophore-related genes in Δ*fur* and Δ*rpoS* mutants. Strains were cultivated in MM at pH 7.5 (dark red), 6.5 (medium red), or 5.5 (light red). GFP-fluorescence emission data, normalized to optical density at 600 nm (OD_{600nm}) of the culture, are shown as the maximum fluorescence per OD_{600nm}. Each point represents one biological replicate (n = 3). **B**. Expression of the iron deprivation marker *ryhB2* (P_{ryhB2}). **C.** Expression of the operon involved in endogenous siderophore biosynthesis *entCEBAH* ($P_{entCEBAH}$). **D.** Expression of the transporter of ENT *fepA* (P_{fepA}). **E.** Expression of the transporter of ferrioxamine E *foxA* (P_{foxA}). Statistical analysis was performed using unpaired t-test (A) or one-way ANOVA followed by Tukey's multiple comparisons test (B). Exact p-values are reported for all comparisons with $p < 0.05$ considered statistically significant.

395

396 **Discussion**

397 For successful growth, organisms must adapt to their environments. Given the crucial
398 role of iron for growth, the regulation of iron acquisition systems in bacteria must be finely
399 tuned. This is especially critical for pathogens that need to establish infection in environments
400 that are already colonized. This study explored how environmental changes, particularly a
401 decrease in pH, influence the utilization of siderophores by *Salmonella*.

402 Our competition assays revealed that under acidic conditions, *Salmonella* benefits more
403 from exploiting exogenous hydroxamate-type siderophores than it does at neutral pH,
404 suggesting this as an adaptive strategy to acidic environments. This increased reliance on
405 exogenous siderophores is linked to a stark reduction in the production of endogenous
406 siderophores, monitored in various *Salmonella* strains (fig. S7), highlighting a drastic
407 adaptation of siderophore production to varying pH changes. This phenomenon has been
408 documented in previous studies. For instance, Valdebenito et *al*., demonstrated that
409 in *Escherichia* coli, the production of ENT decreases under acidic conditions[48]. However, this
410 strain, in contrast to our *Salmonella* strain, is also capable of producing other siderophores,
411 such as aerobactin and yersiniabactin. Aerobactin, a mixed hydroxy acid and hydroxamate-
412 type siderophore, reaches peak production at acidic pH, while yersiniabactin, a phenolate-type
413 siderophore, is maximally produced at alkaline pH 8.5. This indicates that siderophore
414 production in *E. coli* is highly influenced by environmental pH and varies with the type of
415 siderophore[48].

416 In addition to affecting siderophore production, environmental pH can also drive
417 bacterial adaptation at the level of siderophore transport. Li et *al*., found that *Acinetobacter*
418 *baumannii* adapts to pH changes through mutations in the siderophore receptor gene *bauA*[51].

419 This adaptation allows *A. baumannii* to optimize iron uptake and maintain iron levels under
420 varying pH conditions. To explore whether a similar pH-dependent adaptation occurs
421 in *Salmonella*, we investigated how pH affects the affinity of ferrioxamine for its transporter
422 FoxA. However, our results revealed no significant change in ferrioxamine binding to FoxA
423 across different pH levels (Fig. S4).

424 Not only can pH affect the affinity of siderophores for their transporter, but it also
425 influences their affinity for iron by modifying their chelating properties. ENT, a catecholate-
426 type siderophore, is known to have the highest iron affinity at neutral pH (pFe at pH 7.5 = 35)
427 among all the siderophores described[67]. However, Valdebenito et *al*., found that this affinity
428 decreases under acidic conditions (pFe at pH 5.5 = 25). In contrast, hydroxamate siderophores
429 like deferoxamine maintain relatively stable iron affinities across different pH levels (pFe-pH
430 7.5 = 27 and pFe pH-5.5 = 22)[48]. Our competition assays, where ENT and DFOE were added
431 simultaneously at equal concentration, revealed that *Salmonella* favors ENT over DFOE even
432 under acidic conditions. The superior iron-binding capacity of ENT makes it the preferred
433 siderophore when both are available, underlining yet again that the stark dependency on
434 exogenous siderophore at acidic pH is solely due to reduced ENT/SLC production.

435 Upon exposure to low pH, *Salmonella* activates the alternative sigma factor RpoS,
436 which orchestrates the acid tolerance response by upregulating the expression of numerous
437 acid shock proteins but also altering nutrient acquisition, thereby enabling the pathogen to
438 survive in acidic environments[61] . Our data suggest that in acidic environments, RpoS but not
439 Fur reduces siderophore production and thereby increases *Salmonella's* reliance to exogenous
440 siderophores. The exploitation of exogenous siderophores may allow *Salmonella* to avoid the
441 energy costs associated with producing its own siderophores. This emphasis on energy
442 conservation likely explains why the deletion of *rpoS* positively impacts endogenous

443 siderophore production. The loss of RpoS has already been shown to enhance *Salmonella*'s
444 ability to scavenge for limited nutrients[68]. While this strategy may be less critical at neutral pH,
445 it may become especially important under acidic conditions, where conserving energy is vital
446 for enduring the environmental stress and represent an evolutive response to stress conditions.

447 Understanding the conditions under which *Salmonella* utilizes endogenous or
448 exogenous siderophores can provide critical insights for designing targeted therapies. Despite
449 the challenges in pinpointing specific targets, knowing how *Salmonella* adapts its iron
450 acquisition strategies offers valuable information for developing effective treatments. Future
451 research should focus on exploring other environmental clues that could affect iron acquisition
452 mechanisms and thereby offering a better understanding versatility of *Salmonella's* iron uptake
453 strategies and thereby informing future therapeutic approaches.

454 **Acknowledgments:** We are indebted to members of the MMBCA lab for discussion. Thank
455 you to Dr. Connor Sharp for his guidance for the bioinformatic analysis. We thank Prof. Kevin
456 Foster for sharing *Salmonella* strains. **Funding:** MF was supported by an MRT Studentship.
457 This work was supported by IdEx 2022 "Attractivité" University of Strasbourg and the ANR
458 "ANR-24-CE15-7754 – SidExPat" **Author contributions:** Conceptualisation: OC.
459 Methodology: MF and OC. Investigation: MF and OC. Visualisation: MF and OC. Funding
460 acquisition: OC. Supervision: OC and IJS. Writing – original draft: MF and OC. Writing –
461 review and editing: MF, IJS and OC. ChatGPT version 4.o was sometimes used for Language
462 improvement of the manuscript. **Competing interests:** None. **Data and materials**
463 **availability:** All data are available in the main text or supplementary materials and on
464 https://doi.org/10.5281/zenodo.15276328.

465 **Materials and methods**

466 **Bacterial strains and growth conditions** A full list of all bacterial strains used in this study
467 is provided in sup. table S1. *Salmonella* strains used were based on sME51, a prototrophic
468 *hisG*^{Leu69} derivative of *Salmonella enterica* serovar Typhimurium SL1344[69]. All strains were
469 cultivated in Lysogeny Broth (LB) (10 g/L tryptone, 5 g/L yeast extract, 5 g/L NaCl) or
470 Minimal Medium (MM) (15 mM NH_4Cl, 1.5 mM K_2SO_4, 3 mM KH_2PO_4, 1 mM $MgCl_2$, 0.4%
471 glycerol). For pH adjustments, 100 mM HEPES was used to achieve pH 7.5, while 100 mM
472 MES was used for pH 6.5 and 5.5 and filter-sterilized. Media were supplemented with 90 µg/ml
473 streptomycin, and 50 µg/ml kanamycin was added when a plasmid reporter was present.
474 *Escherichia coli* JKe201 was grown in LB supplemented with 100 µM diaminopimelic acid
475 (DAP), and 50 µg/ml kanamycin was added when required. Cultures were incubated at 37°C
476 with shaking at 220 rpm.

477 **Plasmids and genetic engineering of bacterial strains** All primers and plasmids used in this
478 study are listed in sup. table S2 and S3. All plasmids used in this study are low-copy plasmids
479 and carried a kanamycin resistance cassette to ensure their maintenance in bacterial cells. Gene
480 reporter plasmids contained candidate gene promoters fused to a *gfp-ova* reporter to assess
481 specific gene expression in response to experimental conditions as described here[59,60]. For
482 strain differentiation during competition assays, low-copy episomal pSC101-derivatives were
483 employed. These plasmids enabled the constitutive expression of either dTomato or YPet from
484 the P_{ybaJ} promoter, which facilitated tracking the proportions of different strains[59,69]. Gene
485 deletions were obtain using two consecutive single-crossovers, incorporating positive selection
486 for kanamycin resistance and a double negative selection against SacB levan sucrase-mediated
487 sensitivity to sucrose and the expression of the I-SceI endonuclease[70]. The engineered strains
488 preserved a nonapeptide with the first five and last four amino acids, including the stop codon,
489 as described here[70].

490 **Prevalence of siderophore-related genes and phylogenetic analysis in *Salmonella*** To
491 analyze siderophore transporter genes across *Salmonella* strains, we followed a structured
492 bioinformatics workflow. Initially, we sorted and downloaded genomes from the BV-BRC
493 database[55]. Genomes were first assessed for contamination and metadata. We then filtered these
494 genomes to retain only those with a minimum size of 4 million base pairs. To ensure the most
495 representative dataset, we grouped strains by their unique multilocus sequence typing (MLST)
496 type and randomly selected one strain per group using Python's *random.choice ()* function.
497 This approach allowed us to capture the diversity of *Salmonella* strains effectively and resulted
498 in a final dataset of 183 strains, selected from an initial set of 1,146 isolates. For gene detection,
499 we used the ABRicate tool[71] with a custom database to identify specific siderophore-related
500 genes in the genome sequences. Genes were considered present only if they met the default
501 ABRicate thresolds of at least 75% identity and 60% coverage; any gene below these thresholds
502 was classified as absent. Phylogenetic analysis was conducted using PhyloPhlAn[72]. We first
503 generated a database of core proteins for *Salmonella* and then reconstructed the phylogenetic
504 tree by trimming sequences, filtering data, and using FastTree and RAxML for tree
505 construction. Maximum likelihood trees were inferred using concatenated gene sequences with
506 the GTR model and bootstrap support. The resulting tree was visualized and further modified
507 using iTOL (version 7.0) to enhance clarity and presentation.

508 **Competition assays** The competing strains carried a low-plasmid with constitutive expression
509 of fluorescent proteins (YPet or dTomato). Pre-cultures were grown overnight in MM at pH
510 7.5 with 10 μM iron, at 37°C with agitation (220 rpm). Post-incubation, 1 mL of each culture
511 was centrifuged at 9000 rpm for 2 minutes, washed twice with 1X phosphate-buffered saline
512 (PBS), and resuspended to an optical density at 600 nm of 0.1 in 1 mL of 1X PBS. Equal
513 volumes (500 μL each) of the two strains were mixed to create a 1:1 bacterial suspension at
514 OD_{600nm} of 0.1 (OD 0.05 per strain). Fourteen-milliliter tubes containing 1.8 mL of MM at pH

515 7.5, 6.5, or 5.5, with or without exogenous siderophore (all chemicals are reported in sup. table
516 S4), were inoculated with 200 µL of the bacterial mixture to achieve a final OD_{600nm} of 10^{-6}.
517 Cultures were grown for 48 hours at 37°C with agitation (220 rpm). The total number of cells
518 for each strain was determined by plating on LB agar supplemented with 90 µg/mL
519 streptomycin and enumerating colonies under blue light to distinguish the fluorescent proteins.
520 The competitiveness index (CI) was calculated as CI = output/input, where output is the ratio
521 of mutant to wild-type colonies after 48 hours, and input is the ratio at time zero.

522 **Quantification of GFP-fluorescence intensity** Overnight cultures in MM at pH 7.5 with 10
523 µM iron were grown at 37°C with shaking (220 rpm). Following centrifugation (9000 rpm, 2
524 minutes) and washing twice with 1X PBS, cells were resuspended to an OD_{600nm} of 0.1 in 1X
525 PBS. Twenty microliters of this suspension were added to 180 µL of fresh MM at various pH
526 levels (7.5, 6.5, 5.5) with or without iron or exogenous siderophore in a 96-well plate (Greiner,
527 U-bottomed microplate). The plate was incubated at 37°C with shaking in a Tecan microplate
528 reader (Infinite M200, Tecan), with OD_{600nm}, GFP (excitation/emission: 488 nm/510 nm), and
529 mCherry (excitation/emission: 570 nm/610 nm) fluorescence measured every 10 minutes for
530 48 hours. Results from three biological replicates were analyzed, with GFP fluorescence
531 normalized to OD_{600nm} and the maximum value of this normalization used for histograms.
532 Statistical significance was determined with p-values <0.05.

533 **Ligand binding assay** To determine the dissociation constant (Kd) between Ferri-DFOE and
534 its transporter FoxA in *Salmonella*, strains were cultured overnight in MM at pH 7.5 or 5.5,
535 with 10 µM DFOE added to induce FoxA transporter expression. Complexes of $^{55}FeCl_3$-DFOE
536 were prepared with a ^{55}Fe concentration of 20 µM and a siderophore ratio of 20:1. A known
537 concentration of *Salmonella* was incubated with $^{55}FeCl_3$-DFOE complexes in cold-buffer at
538 pH 7.5 (100 mM HEPES) or pH 5.5 (100 mM MES) for 1 hour at 0°C, with transport inhibited

539 by adding Carbonyl cyanide 3-chlorophenylhydrazone. Bacterial cells bound to the complexes
540 were recovered by filtration using a Brandel filtration system (M-48 Cell Harvester) and
541 Whatman® glass microfiber filters (Grade GF/B, 460x570 mm). Radioactivity associated with
542 the bacteria was measured with a scintillation counter to calculate the K*d*. This binding assay
543 was conducted in triplicate.

544 **Siderophore production** Overnight cultures grown in MM at pH 7.5 with 10 µM iron were
545 pelleted, re-suspended in fresh MM at pH 7.5 or 5.5 to an OD_{600nm} of 0.01, and incubated with
546 shaking at 37°C for 24 hours. The OD_{600nm} was measured to assess cell growth. Supernatants
547 were analyzed by UV-Vis spectroscopy. Preliminary, calibration curves with pure ENT and its
548 degradation product, DHBS, were established, with absorbance peaks at 330 nm for ENT and
549 310 nm for DHBS at pH 7.5, and at 317 nm for ENT and 310 nm for DHBS at pH 5.5. Molar
550 extinction coefficients were εENT pH 7.5 = 8100 $M^{-1}.cm^{-1}$, εENT pH 5.5 = 2290 $M^{-1}.cm^{-1}$,
551 εDHBS pH 7.5 = 7000 $M^{-1}.cm^{-1}$, and εDHBS pH 5.5 = 2100 $M^{-1}.cm^{-1}$. Absorbance monitored
552 from supernatants were normalized to OD_{600nm} of the cultures. Control experiments compared
553 the absorbance of ENT/DHBS in wild-type strains with those deleted for siderophore
554 production to account for interference from other media components.

555 **Statistics** Statistical tests were performed with GraphPad Prism (version 10.2.3) as indicated
556 in the figure legends. Figure legends indicate the statistical tests used with all biological
557 replicates depicted in the figures.

558

559 **References**

560 1. Cairo, G., Bernuzzi, F., and Recalcati, S. (2006). A precious metal: Iron, an essential
561 nutrient for all cells. Genes Nutr *1*, 25–39. https://doi.org/10.1007/BF02829934.
562 2. Cook, J.D., Skikne, B.S., Lynch, S.R., and Reusser, M.E. (1986). Estimates of iron
563 sufficiency in the US population. Blood *68*, 726–731.

564 3. Błażewicz, A., Klatka, M., Astel, A., Partyka, M., and Kocjan, R. (2013). Differences
565 in trace metal concentrations (Co, Cu, Fe, Mn, Zn, Cd, And Ni) in whole blood, plasma, and
566 urine of obese and nonobese children. Biol Trace Elem Res *155*, 190–200.
567 https://doi.org/10.1007/s12011-013-9783-8.
568 4. Palmer, L.D., and Skaar, E.P. (2016). Transition Metals and Virulence in Bacteria.
569 Annu. Rev. Genet. *50*, 67–91. https://doi.org/10.1146/annurev-genet-120215-035146.
570 5. Yeh, K., Yeh, M., and Glass, J. (2004). Hepcidin regulation of ferroportin 1 expression
571 in the liver and intestine of the rat. American Journal of Physiology-Gastrointestinal and Liver
572 Physiology *286*, G385–G394. https://doi.org/10.1152/ajpgi.00246.2003.
573 6. Flo, T.H., Smith, K.D., Sato, S., Rodriguez, D.J., Holmes, M.A., Strong, R.K., Akira,
574 S., and Aderem, A. (2004). Lipocalin 2 mediates an innate immune response to bacterial
575 infection by sequestrating iron. Nature *432*, 917–921. https://doi.org/10.1038/nature03104.
576 7. Gao, H., and Bian, X. (2022). Editorial: Microbial Siderophores: Biosynthesis,
577 Regulation, and Physiological and Ecological Impacts. Front Microbiol *13*, 892485.
578 https://doi.org/10.3389/fmicb.2022.892485.
579 8. Schalk, I.J. (2025). Bacterial siderophores: diversity, uptake pathways and applications.
580 Nat Rev Microbiol *23*, 24–40. https://doi.org/10.1038/s41579-024-01090-6.
581 9. Schalk, I.J., Mislin, G.L.A., and Brillet, K. (2012). Structure, Function and Binding
582 Selectivity and Stereoselectivity of Siderophore–Iron Outer Membrane Transporters. Current
583 Topics in Membranes *69*, 37–66. https://doi.org/10.1016/B978-0-12-394390-3.00002-1.
584 10. Deriu, E., Liu, J.Z., Pezeshki, M., Edwards, R.A., Ochoa, R.J., Contreras, H., Libby,
585 S.J., Fang, F.C., and Raffatellu, M. (2013). Probiotic bacteria reduce salmonella typhimurium
586 intestinal colonization by competing for iron. Cell Host Microbe *14*, 26–37.
587 https://doi.org/10.1016/j.chom.2013.06.007.
588 11. Singh, V., Yeoh, B.S., Xiao, X., Kumar, M., Bachman, M., Borregaard, N., Joe, B., and
589 Vijay-Kumar, M. (2015). Interplay between enterobactin, myeloperoxidase and lipocalin 2
590 regulates E. coli survival in the inflamed gut. Nat Commun *6*, 7113.
591 https://doi.org/10.1038/ncomms8113.
592 12. Raffatellu, M., George, M.D., Akiyama, Y., Hornsby, M.J., Nuccio, S.-P., Paixao, T.A.,
593 Butler, B.P., Chu, H., Santos, R.L., Berger, T., et al. (2009). Lipocalin-2 Resistance Confers
594 an Advantage to Salmonella enterica Serotype Typhimurium for Growth and Survival in the
595 Inflamed Intestine. Cell Host & Microbe *5*, 476–486.
596 https://doi.org/10.1016/j.chom.2009.03.011.
597 13. Cunrath, O., and Palmer, J.D. (2021). An overview of Salmonella enterica metal

598 homeostasis pathways during infection. Microlife *2*, uqab001.
599 https://doi.org/10.1093/femsml/uqab001.
600 14. Aisen, P., and Leibman, A. (1972). Lactoferrin and transferrin: a comparative study.
601 Biochim Biophys Acta *257*, 314–323. https://doi.org/10.1016/0005-2795(72)90283-8.
602 15. Mazurier, J., and Spik, G. (1980). Comparative study of the iron-binding properties of
603 human transferrins. I. Complete and sequential iron saturation and desaturation of the
604 lactotransferrin. Biochim Biophys Acta *629*, 399–408. https://doi.org/10.1016/0304-
605 4165(80)90112-9.
606 16. Nakashige, T.G., Zhang, B., Krebs, C., and Nolan, E.M. (2015). Human calprotectin is
607 an iron-sequestering host-defense protein. Nat Chem Biol *11*, 765–771.
608 https://doi.org/10.1038/nchembio.1891.
609 17. Goetz, D.H., Holmes, M.A., Borregaard, N., Bluhm, M.E., Raymond, K.N., and Strong,
610 R.K. (2002). The neutrophil lipocalin NGAL is a bacteriostatic agent that interferes with
611 siderophore-mediated iron acquisition. Mol Cell *10*, 1033–1043.
612 https://doi.org/10.1016/s1097-2765(02)00708-6.
613 18. Vazquez-Gutierrez, P., Lacroix, C., Jaeggi, T., Zeder, C., Zimmerman, M.B., and
614 Chassard, C. (2015). Bifidobacteria strains isolated from stools of iron deficient infants can
615 efficiently sequester iron. BMC Microbiol *15*, 3. https://doi.org/10.1186/s12866-014-0334-z.
616 19. Vazquez-Gutierrez, P., Stevens, M.J.A., Gehrig, P., Barkow-Oesterreicher, S., Lacroix,
617 C., and Chassard, C. (2017). The extracellular proteome of two Bifidobacterium species reveals
618 different adaptation strategies to low iron conditions. BMC Genomics *18*, 41.
619 https://doi.org/10.1186/s12864-016-3472-x.
620 20. Aguiar, M., Orasch, T., Misslinger, M., Dietl, A.-M., Gsaller, F., and Haas, H. (2021).
621 The Siderophore Transporters Sit1 and Sit2 Are Essential for Utilization of Ferrichrome-,
622 Ferrioxamine- and Coprogen-Type Siderophores in Aspergillus fumigatus. J Fungi (Basel) *7*,
623 768. https://doi.org/10.3390/jof7090768.
624 21. Santus, W., Rana, A., Devlin, J., Kiernan, K., Jacob, C., Tjokrosurjo, J., Underhill, D.,
625 and Behnsen, J. (2022). Fungal xenosiderophores from mycobiota and diet promote Salmonella
626 colonization of the inflamed gut (In Review) https://doi.org/10.21203/rs.3.rs-1175303/v1.
627 22. Ong, S.A., and Neilands, J.B. (1979). Siderophores in microbially processed cheese. J
628 Agric Food Chem *27*, 990–995. https://doi.org/10.1021/jf60225a033.
629 23. Luckey, M., Pollack, J.R., Wayne, R., Ames, B.N., and Neilands, J.B. (1972). Iron
630 Uptake in *Salmonella typhimurium* : Utilization of Exogenous Siderochromes as Iron Carriers.
631 J Bacteriol *111*, 731–738. https://doi.org/10.1128/jb.111.3.731-738.1972.

632 24. O'Brien, S., Culbert, C., and Barraclough, T.G. (2022). Public goods exploitation is
633 reduced in species-rich microbial communities. Preprint,
634 https://doi.org/10.1101/2022.11.25.517952 https://doi.org/10.1101/2022.11.25.517952.
635 25. Kramer, J., Özkaya, Ö., and Kümmerli, R. (2020). Bacterial siderophores in community
636 and host interactions. Nat Rev Microbiol *18*, 152–163. https://doi.org/10.1038/s41579-019-
637 0284-4.
638 26. Spiga, L., Fansler, R.T., Perera, Y.R., Shealy, N.G., Munneke, M.J., Torres, T.P.,
639 David, H.E., Lemoff, A., Ran, X., Richardson, K.L., et al. (2023). Iron acquisition by a
640 commensal bacterium modifies host nutritional immunity during *Salmonella* infection
641 (Microbiology) https://doi.org/10.1101/2023.06.25.546471.
642 27. Heymann, P., Gerads, M., Schaller, M., Dromer, F., Winkelmann, G., and Ernst, J.F.
643 (2002). The Siderophore Iron Transporter of *Candida albicans* (Sit1p/Arn1p) Mediates Uptake
644 of Ferrichrome-Type Siderophores and Is Required for Epithelial Invasion. Infect Immun *70*,
645 5246–5255. https://doi.org/10.1128/IAI.70.9.5246-5255.2002.
646 28. Hastie, J.L., Carmichael, H.L., Werner, B.M., Dunbar, K.E., and Carlson, P.E. (2023).
647 *Clostridioides difficile* utilizes siderophores as an iron source and FhuDBGC contributes to
648 ferrichrome uptake. J Bacteriol, e00324-23. https://doi.org/10.1128/jb.00324-23.
649 29. Hartmann, A., and Braun, V. (1980). Iron transport in Escherichia coli: uptake and
650 modification of ferrichrome. J Bacteriol *143*, 246–255. https://doi.org/10.1128/jb.143.1.246-
651 255.1980.
652 30. Pollack, J.R., Ames, B.N., and Neilands, J.B. (1970). Iron Transport in *Salmonella*
653 *typhimurium:* Mutants Blocked in the Biosynthesis of Enterobactin. J Bacteriol *104*, 635–639.
654 https://doi.org/10.1128/jb.104.2.635-639.1970.
655 31. Lundrigan, M.D., and Kadner, R.J. (1986). Nucleotide sequence of the gene for the
656 ferrienterochelin receptor FepA in Escherichia coli. Homology among outer membrane
657 receptors that interact with TonB. J Biol Chem *261*, 10797–10801.
658 32. Fischbach, M.A., Lin, H., Liu, D.R., and Walsh, C.T. (2005). *In vitro* characterization
659 of IroB, a pathogen-associated *C* -glycosyltransferase. Proc. Natl. Acad. Sci. U.S.A. *102*, 571–
660 576. https://doi.org/10.1073/pnas.0408463102.
661 33. Raymond, K.N., Dertz, E.A., and Kim, S.S. (2003). Enterobactin: An archetype for
662 microbial iron transport. Proc. Natl. Acad. Sci. U.S.A. *100*, 3584–3588.
663 https://doi.org/10.1073/pnas.0630018100.
664 34. Loomis, L.D., and Raymond, K.N. (1991). Solution equilibria of enterobactin and
665 metal-enterobactin complexes. Inorg. Chem. *30*, 906–911.

666 https://doi.org/10.1021/ic00005a008.
667 35. Fischbach, M.A., Lin, H., Zhou, L., Yu, Y., Abergel, R.J., Liu, D.R., Raymond, K.N.,
668 Wanner, B.L., Strong, R.K., Walsh, C.T., et al. (2006). The pathogen-associated *iroA* gene
669 cluster mediates bacterial evasion of lipocalin 2. Proc. Natl. Acad. Sci. U.S.A. *103*, 16502–
670 16507. https://doi.org/10.1073/pnas.0604636103.
671 36. Sauer, M., Hantke, K., and Braun, V. (1987). Ferric-coprogen receptor FhuE of
672 Escherichia coli: processing and sequence common to all TonB-dependent outer membrane
673 receptor proteins. J Bacteriol *169*, 2044–2049. https://doi.org/10.1128/jb.169.5.2044-
674 2049.1987.
675 37. Kingsley, R.A., Reissbrodt, R., Rabsch, W., Ketley, J.M., Tsolis, R.M., Everest, P.,
676 Dougan, G., Bäumler, A.J., Roberts, M., and Williams, P.H. (1999). Ferrioxamine-Mediated
677 Iron(III) Utilization by *Salmonella enterica*. Appl Environ Microbiol *65*, 1610–1618.
678 https://doi.org/10.1128/AEM.65.4.1610-1618.1999.
679 38. Rabsch, W., Voigt, W., Reissbrodt, R., Tsolis, R.M., and Bäumler, A.J. (1999).
680 *Salmonella typhimurium* IroN and FepA Proteins Mediate Uptake of Enterobactin but Differ
681 in Their Specificity for Other Siderophores. J Bacteriol *181*, 3610–3612.
682 https://doi.org/10.1128/JB.181.11.3610-3612.1999.
683 39. Wang, Y., Chen, X., Hu, Y., Zhu, G., White, A.P., and Köster, W. (2018). Evolution
684 and Sequence Diversity of FhuA in Salmonella and Escherichia. Infect Immun *86*, e00573-18.
685 https://doi.org/10.1128/IAI.00573-18.
686 40. Postle, K., and Larsen, R.A. (2007). TonB-dependent energy transduction between
687 outer and cytoplasmic membranes. Biometals *20*, 453–465. https://doi.org/10.1007/s10534-
688 006-9071-6.
689 41. Bäumler, A.J., Norris, T.L., Lasco, T., Voigt, W., Reissbrodt, R., Rabsch, W., and
690 Heffron, F. (1998). IroN, a Novel Outer Membrane Siderophore Receptor Characteristic of
691 *Salmonella enterica*. J Bacteriol *180*, 1446–1453. https://doi.org/10.1128/JB.180.6.1446-
692 1453.1998.
693 42. Hantke, K. (1990). Dihydroxybenzoylserine--a siderophore for E. coli. FEMS
694 Microbiol Lett *55*, 5–8. https://doi.org/10.1016/0378-1097(90)90158-m.
695 43. Schwarzenbach, G., and Schwarzenbach, K. (1963). Hydroxamatkomplexe I. Die
696 Stabilität der Eisen(III)-Komplexe einfacher Hydroxamsäuren und des Ferrioxamins B.
697 Helvetica Chimica Acta *46*, 1390–1400. https://doi.org/10.1002/hlca.19630460434.
698 44. Wong, G.B., Kappel, M.J., Raymond, K.N., Matzanke, B., and Winkelmann, G. (1983).
699 Coordination chemistry of microbial iron transport compounds. 24. Characterization of

700 coprogen and ferricrocin, two ferric hydroxamate siderophores. J. Am. Chem. Soc. *105*, 810–
701 815. https://doi.org/10.1021/ja00342a027.
702 45. Anderegg, G., L'Eplattenier, F., and Schwarzenbach, G. (1963). Hydroxamatkomplexe
703 II. Die Anwendung der pH-Methode. Helv. Chim. Acta *46*, 1400–1408.
704 https://doi.org/10.1002/hlca.19630460435.
705 46. Bagg, A., and Neilands, J.B. (1987). Ferric uptake regulation protein acts as a repressor,
706 employing iron(II) as a cofactor to bind the operator of an iron transport operon in Escherichia
707 coli. Biochemistry *26*, 5471–5477. https://doi.org/10.1021/bi00391a039.
708 47. Saldaña-Ahuactzi, Z., and Knodler, L.A. FoxR is an AraC-like transcriptional regulator
709 of ferrioxamine uptake in Salmonella enterica. Molecular Microbiology *n/a*.
710 https://doi.org/10.1111/mmi.14970.
711 48. Valdebenito, M., Crumbliss, A.L., Winkelmann, G., and Hantke, K. (2006).
712 Environmental factors influence the production of enterobactin, salmochelin, aerobactin, and
713 yersiniabactin in Escherichia coli strain Nissle 1917. International Journal of Medical
714 Microbiology *296*, 513–520. https://doi.org/10.1016/j.ijmm.2006.06.003.
715 49. Maurer, J.M., Schellekens, R.C.A., Van Rieke, H.M., Wanke, C., Iordanov, V.,
716 Stellaard, F., Wutzke, K.D., Dijkstra, G., Van Der Zee, M., Woerdenbag, H.J., et al. (2015).
717 Gastrointestinal pH and Transit Time Profiling in Healthy Volunteers Using the IntelliCap
718 System Confirms Ileo-Colonic Release of ColoPulse Tablets. PLoS ONE *10*, e0129076.
719 https://doi.org/10.1371/journal.pone.0129076.
720 50. McNeil, N.I., Ling, K.L., and Wager, J. (1987). Mucosal surface pH of the large
721 intestine of the rat and of normal and inflamed large intestine in man. Gut *28*, 707–713.
722 https://doi.org/10.1136/gut.28.6.707.
723 51. Li, T., Luo, D., Ning, N., Liu, X., Chen, F., Zhang, L., Bao, C., Li, Z., Li, D., Gu, H.,
724 et al. (2023). *Acinetobacter baumannii* adaptation to the host pH microenvironment is mediated
725 by allelic variation in a single residue of BauA protein. PNAS Nexus *2*, pgad079.
726 https://doi.org/10.1093/pnasnexus/pgad079.
727 52. O'Brien, S., Culbert, C.T., and Barraclough, T.G. (2023). Community composition
728 drives siderophore dynamics in multispecies bacterial communities. BMC Ecol Evol *23*, 45.
729 https://doi.org/10.1186/s12862-023-02152-8.
730 53. Gräff, Á.T., and Barry, S.M. (2024). Siderophores as tools and treatments. NPJ
731 Antimicrob Resist *2*, 47. https://doi.org/10.1038/s44259-024-00053-4.
732 54. Shao, J., Rong, N., Wu, Z., Gu, S., Liu, B., Shen, N., and Li, Z. (2023). Siderophore-
733 mediated iron partition promotes dynamical coexistence between cooperators and cheaters.

iScience *26*, 107396. https://doi.org/10.1016/j.isci.2023.107396.

55. Wattam, A.R., Davis, J.J., Assaf, R., Boisvert, S., Brettin, T., Bun, C., Conrad, N., Dietrich, E.M., Disz, T., Gabbard, J.L., et al. (2017). Improvements to PATRIC, the all-bacterial Bioinformatics Database and Analysis Resource Center. Nucleic Acids Res *45*, D535–D542. https://doi.org/10.1093/nar/gkw1017.

56. Albrecht-Gary, A.M., and Crumbliss, A.L. (1998). Coordination chemistry of siderophores: thermodynamics and kinetics of iron chelation and release. Met Ions Biol Syst *35*, 239–327.

57. Ihnat, P.M., Vennerstrom, J.L., and Robinson, D.H. (2002). Solution equilibria of deferoxamine amides. Journal of Pharmaceutical Sciences *91*, 1733–1741. https://doi.org/10.1002/jps.10168.

58. Hoegy, F., Celia, H., Mislin, G.L., Vincent, M., Gallay, J., and Schalk, I.J. (2005). Binding of Iron-free Siderophore, a Common Feature of Siderophore Outer Membrane Transporters of Escherichia coli and Pseudomonas aeruginosa. Journal of Biological Chemistry *280*, 20222–20230. https://doi.org/10.1074/jbc.M500776200.

59. Cunrath, O., and Bumann, D. (2019). Host resistance factor SLC11A1 restricts *Salmonella* growth through magnesium deprivation. Science *366*, 995–999. https://doi.org/10.1126/science.aax7898.

60. Ferry, M., Ferriz, H., Sharp, C., Paschalidis, C., Boutant, E., Schalk, I.J., and Cunrath, O. (2024). Characterisation of *Pseudomonas aeruginosa's* metal-responsive TonB-dependent transporters. Preprint, https://doi.org/10.1101/2024.10.14.618150 https://doi.org/10.1101/2024.10.14.618150.

61. Kehres, D.G., Janakiraman, A., Slauch, J.M., and Maguire, M.E. (2002). SitABCD Is the Alkaline Mn^{2+} Transporter of *Salmonella enterica* Serovar Typhimurium. J Bacteriol *184*, 3159–3166. https://doi.org/10.1128/JB.184.12.3159-3166.2002.

62. Makui, H., Roig, E., Cole, S.T., Helmann, J.D., Gros, P., and Cellier, M.F.M. (2000). Identification of the *Escherichia coli* K-12 Nramp orthologue (MntH) as a selective divalent metal ion transporter. Molecular Microbiology *35*, 1065–1078. https://doi.org/10.1046/j.1365-2958.2000.01774.x.

63. Hantke, K. (2003). Is the bacterial ferrous iron transporter FeoB a living fossil? Trends in Microbiology *11*, 192–195. https://doi.org/10.1016/S0966-842X(03)00100-8.

64. Soo Lee, I., Lin, J., Hall, H.K., Bearson, B., and Foster, J.W. (1995). The stationary-phase sigma factor ? ^{S} (RpoS) is required for a sustained acid tolerance response in virulent Salmonella typhimurium. Mol Microbiol *17*, 155–167. https://doi.org/10.1111/j.1365-

768 2958.1995.mmi_17010155.x.
769 65. Lange, R., and Hengge-Aronis, R. (1991). Identification of a central regulator of
770 stationary-phase gene expression in Escherichia coli. Mol Microbiol *5*, 49–59.
771 https://doi.org/10.1111/j.1365-2958.1991.tb01825.x.
772 66. Hall, H.K., and Foster, J.W. (1996). The role of fur in the acid tolerance response of
773 Salmonella typhimurium is physiologically and genetically separable from its role in iron
774 acquisition. J Bacteriol *178*, 5683–5691. https://doi.org/10.1128/jb.178.19.5683-5691.1996.
775 67. Harris, W.R., Carrano, C.J., Cooper, S.R., Sofen, S.R., Avdeef, A.E., McArdle, J.V.,
776 and Raymond, K.N. (1979). Coordination chemistry of microbial iron transport compounds.
777 19. Stability constants and electrochemical behavior of ferric enterobactin and model
778 complexes. J. Am. Chem. Soc. *101*, 6097–6104. https://doi.org/10.1021/ja00514a037.
779 68. Notley-McRobb, L., King, T., and Ferenci, T. (2002). rpoS mutations and loss of
780 general stress resistance in Escherichia coli populations as a consequence of conflict between
781 competing stress responses. J Bacteriol *184*, 806–811. https://doi.org/10.1128/JB.184.3.806-
782 811.2002.
783 69. Claudi, B., Spröte, P., Chirkova, A., Personnic, N., Zankl, J., Schürmann, N., Schmidt,
784 A., and Bumann, D. (2014). Phenotypic Variation of Salmonella in Host Tissues Delays
785 Eradication by Antimicrobial Chemotherapy. Cell *158*, 722–733.
786 https://doi.org/10.1016/j.cell.2014.06.045.
787 70. Cianfanelli, F.R., Cunrath, O., and Bumann, D. (2020). Efficient dual-negative
788 selection for bacterial genome editing. BMC Microbiol *20*, 129.
789 https://doi.org/10.1186/s12866-020-01819-2.
790 71. Seemann, T. (2025). tseemann/abricate.
791 72. Asnicar, F., Thomas, A.M., Beghini, F., Mengoni, C., Manara, S., Manghi, P., Zhu, Q.,
792 Bolzan, M., Cumbo, F., May, U., et al. (2020). Precise phylogenetic analysis of microbial
793 isolates and genomes from metagenomes using PhyloPhlAn 3.0. Nat Commun *11*, 2500.
794 https://doi.org/10.1038/s41467-020-16366-7.
795
796
797
798
799

Supplementary figures

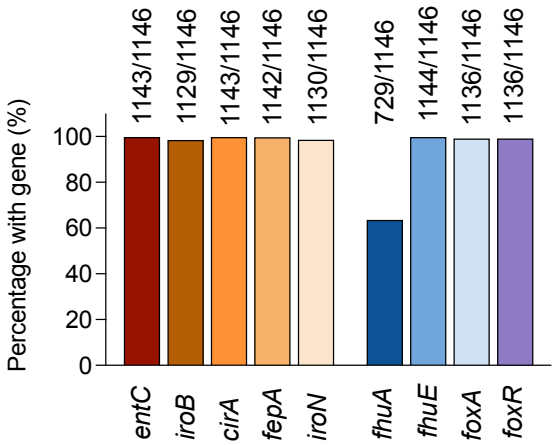

Fig. S1. Conservation of siderophore-related genes among 1,146 *Salmonella* strains from the BV-BRC database. Bars in warm colours indicate the proportion of tested strains carrying genes involved in endogenous siderophore biosynthesis (*entC*, *iroB*) and uptake (*cirA*, *fepA*, *iroN*). Bars in cool colors indicate the proportion of tested strains carrying genes involved in exogenous siderophore uptake (*fhuA*, *fhuE* and *foxA*) and its regulation (*foxR*). These isolates were selected following a structured bioinformatics workflow, which included genome quality assessment, contamination checks, and filtering based on a minimum genome size of 4 million base pairs (see Methods).

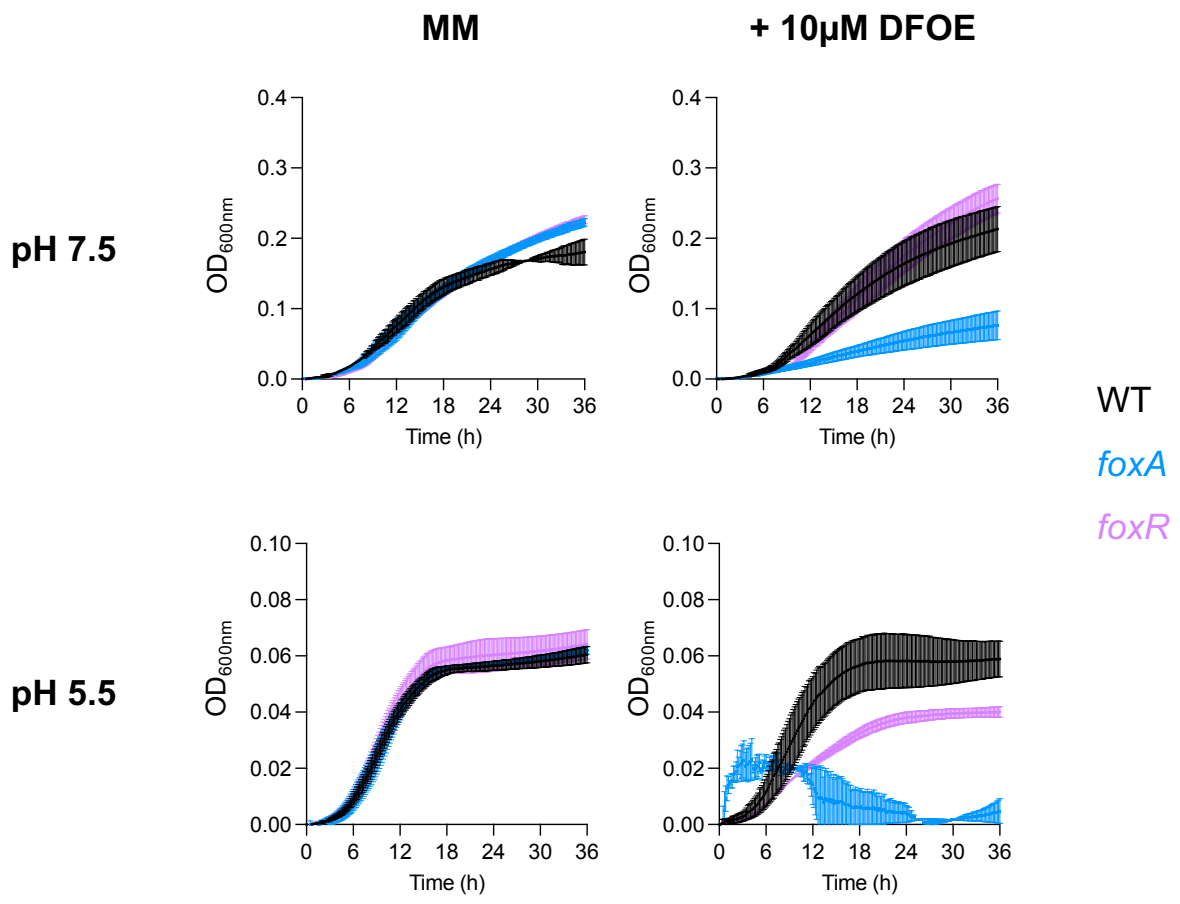

Fig. S2. *Salmonella* WT DFOE-dependent growth kinetics at various pH (7.5 vs 5.5). Bacterial strains were cultivated in iron-depleted medium at either neutral (pH 7.5) or acidic (pH 5.5) conditions, in the absence or presence of 10 µM of DFOE. Growth was initiated at an OD_{600nm} of 0.01 and monitored over time. The WT strain (black) was compared to the *foxA* deletion mutant (blue) which cannot exploit DFOE, and the *foxR* deletion mutant (purple), which is unable to regulate *foxA* expression in response to DFOE. Each growth curve represents the median with the standard error of mean of three biological replicates.

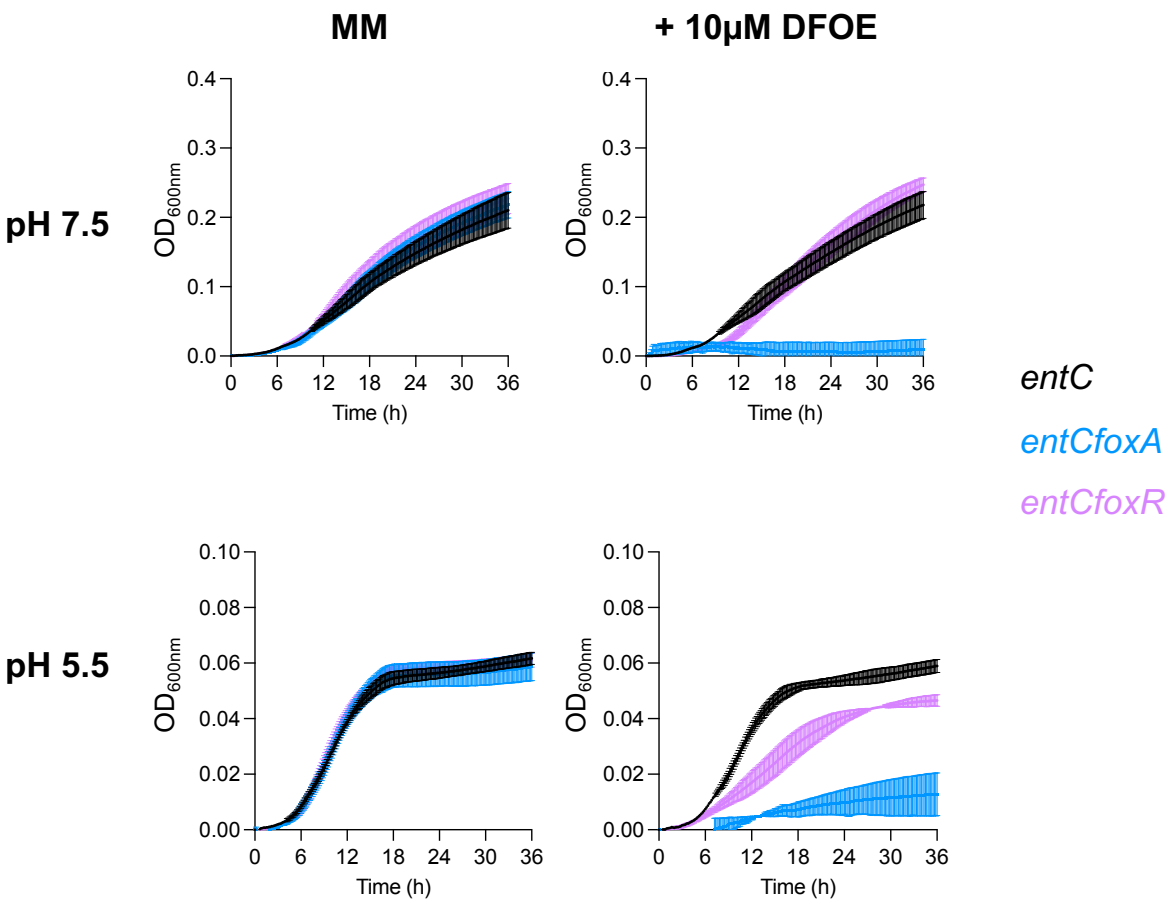

Fig. S3. *Salmonella entC* mutant DFOE-dependent growth kinetics at various pH (7.5 vs 5.5). Bacterial strains were cultivated in iron-depleted medium at either neutral (pH 7.5) or acidic (pH 5.5) conditions, in the absence or presence of 10 µM of DFOE. Growth was initiated at an OD_{600nm} of 0.01 and monitored over time. The *entC* mutant (black), which cannot produce endogenous siderophores but can exploit DFOE, was compared to the *entCfoxA* double mutant (blue), which lacks both endogenous siderophore production and the ability to exploit DFOE, and the *entCfoxR* double mutant (purple), which lacks endogenous siderophore production and cannot regulate *foxA* expression in response to DFOE. Each growth curve represents the median with the standard error of mean of three biological replicates.

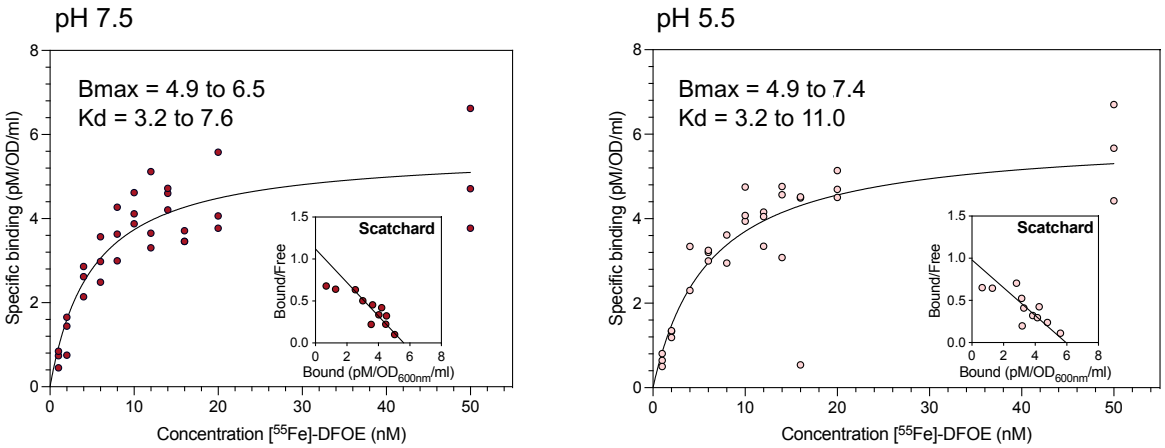

Fig. S4. Binding of Fe-DFOE to FoxA in *Salmonella* in function of the pH (7.5 vs 5.5). Bacterial cells were incubated with a series of concentrations of [^{55}Fe]-DFOE at 0°C for 1 hour in HEPES buffer (pH 7.5) or MES buffer (pH 5.5), with transport inhibited by carbonyl cyanide 3-chlorophenylhydrazone (CCCP). [^{55}Fe]-DFOE binding was assessed by filtration and radioactivity associated with the cells was measured by scintillation counting to determine the dissociation constant (K*d*) and the maximum binding capacity (Bmax). The saturation binding curves represent the specific binding of Fe-DFOE to FoxA at both pH conditions. Inset, Scatchard analysis of specific binding. Each data point represents one biological replicate (n = 3).

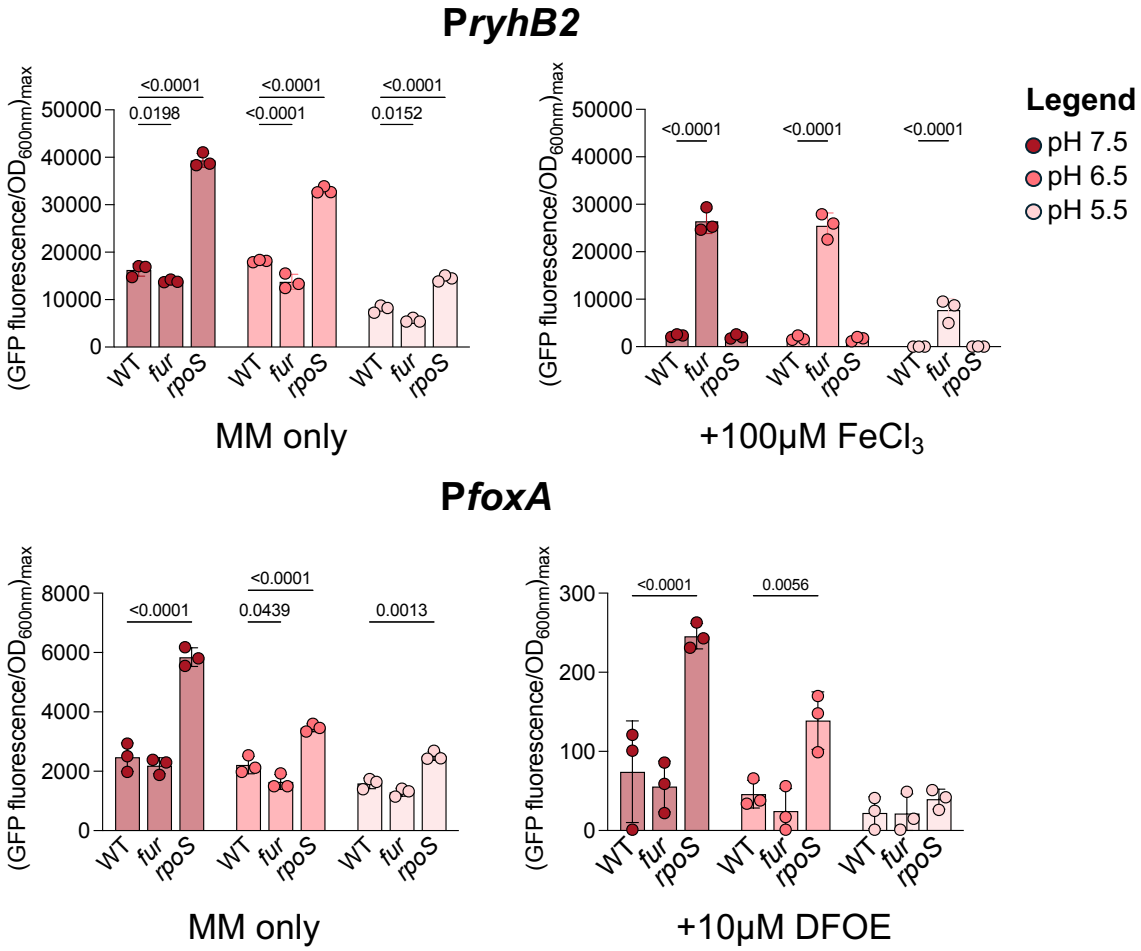

Fig. S5. Transcriptional expression of *ryhB2* (P_{ryhB2}) and *foxA* (P_{foxA}) in *Salmonella* at different pH levels, in iron-poor and iron-supplemented medium. Strains were cultivated in MM under iron-depleted conditions or supplemented with 100 µM $FeCl_3$ (PryhB2) or 10 µM DFOE (PfoxA). Cultures were grown at pH 7.5 (dark red), pH 6.5 (medium red), and pH 5.5 (light red). Fluorescence emission from P*ryhB2-gfp* and P*foxA-gfp* transcriptional reporters, normalized to OD_{600nm}. The maximum fluorescence signal during growth is shown. Expression was compared between the WT strain, a *fur* deletion mutant and a *rpoS* deletion mutant. Each point represents one biological replicate (n = 3). Statistical analysis was performed using one-way ANOVA followed by Tukey's multiple comparisons test. Exact p-values are reported for all comparisons with $p < 0.05$ considered statistically significant.

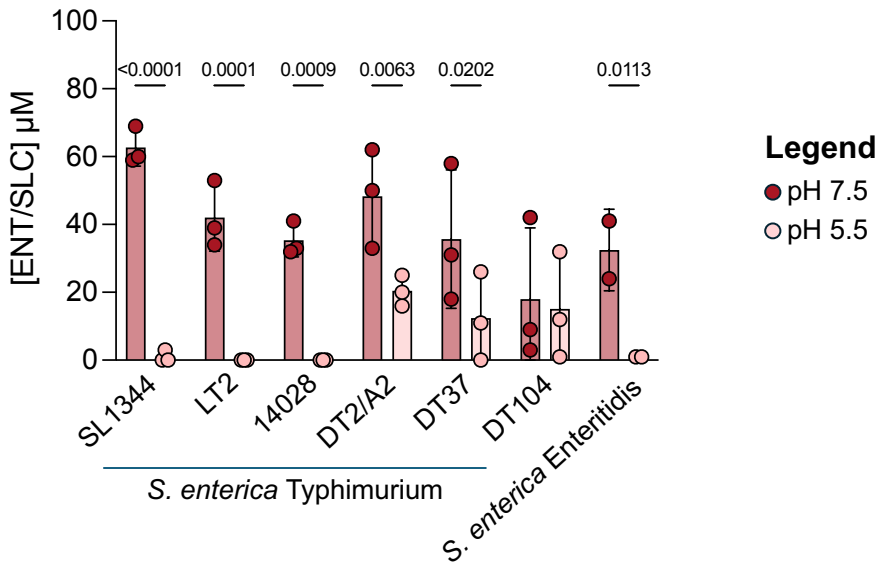

Fig. S6. Endogenous siderophore production (ENT/SLC) by different strains of *S. enterica* in function of pH. Endogenous siderophore concentrations were measured in the supernatant of various *S. enterica* strains after 24 hours of cultivation in MM under iron-depleted at pH 7.5 (dark red) and pH 5.5 (light red). The concentrations of ENT and SLC are shown together as SLC is a glycosylated derivative of ENT. Each point represents one biological replicate (n = 3). Statistical analysis was performed using an unpaired t-test.

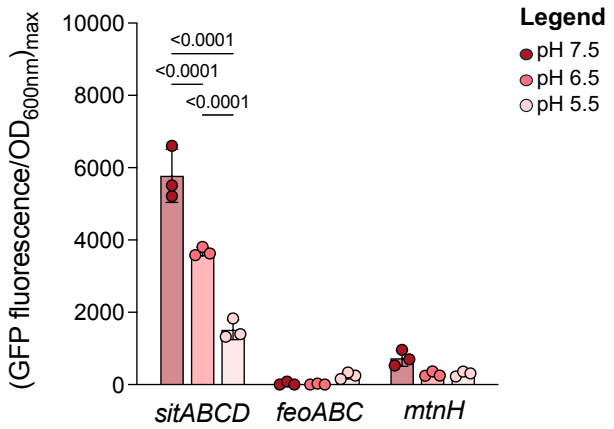

Fig. S7. Transcriptional expression of the ferrous iron uptake systems in *Salmonella* ($P_{sitABCD}$, P_{feoABC} and P_{mntH}) at different pH levels. Strains were cultivated in MM under iron-depleted at pH 7.5 (dark red), pH 6.5 (medium red), and pH 5.5 (light red). Fluorescence emission from P*sitABCD-gfp*, P*feoABC-gfp* and P*mntH-gfp* transcriptional reporters was normalized to OD_{600nm}. The maximum fluorescence signal during growth is shown. Each point represents one biological replicate (n = 3). Statistical analysis was performed using one-way ANOVA followed by Tukey's multiple comparisons test. Exact p-values are reported for all comparisons with $p < 0.05$ considered statistically significant.

873 **Figure captions**

874 Figure 1. Siderophore mediated iron uptake in *Salmonella enterica*.

875 Figure 2. Conservation of siderophore-related genes across *Salmonella enterica* species
876 highlights their ecological importance.

877 Figure 3. The reliance of *Salmonella* on exogenous siderophore exploitation increases in acidic
878 conditions.

879 Figure 4. Endogenous siderophore production decreases in acidic conditions, heightening
880 reliance on exogenous siderophores.

881 Figure 5. Loss of the sigma factor RpoS enhances endogenous siderophore production and
882 acquisition at acidic pH.

883 Fig. S1. Conservation of siderophore-related genes among 1,146 *Salmonella* strains from the
884 BV-BRC database.

885 Fig. S2. *Salmonella* WT DFOE-dependent growth kinetics at various pH (7.5 vs 5.5).

886 Fig. S3. *Salmonella entC* mutant DFOE-dependent growth kinetics at various pH (7.5 vs 5.5).

887 Fig. S4. Binding of Fe-DFOE to FoxA in *Salmonella* in function of the pH (7.5 vs 5.5).

888 Fig. S5. Transcriptional expression of ryhB2 (P*ryhB2*) and foxA (P*foxA*) in *Salmonella* at
889 different pH levels, in iron-poor and iron-supplemented medium.

890 Fig. S6. Endogenous siderophore production (ENT/SLC) by different strains of *S. enterica* in
891 function of pH.

892 Fig. S7. Transcriptional expression of the ferrous iron uptake systems in *Salmonella*
893 (P*sitABCD*, P*feoABC* and P*mntH*) at different pH levels.

894 Tab. S1. Strains used in this study.

895 Tab. S2. Primers used in this study.

896 Tab. S3. Plasmids used in this study.

897 Tab. S4. Reagents used in this study.

898 Tab. S5. Strain information and gene blast results of the 1,186 strains of *Salmonella*. Found on
899 https://doi.org/10.5281/zenodo.15276328